

Visual acuity of fly photoreceptors in natural conditions – dependence on UV sensitizing pigment and light-controlling pupil

Doekele G. Stavenga

Department of Neurobiophysics, University of Groningen, Nijenborgh 4, NL 9747 AG Groningen, The Netherlands

e-mail: stavenga@phys.rug.nl

Accepted 19 February 2004

Summary

The effect of the UV-absorbing sensitizing pigment of fly photoreceptors on absolute, spectral and angular sensitivity was investigated with a wave-optics model for the facet lens–rhabdomere system. When sky light was used as a UV-rich light source, one sensitizing pigment molecule per rhodopsin increased the photoreceptor absorption by 14–18% with respect to pure rhodopsin, whilst two sensitizing pigment molecules per rhodopsin increased the absorption by 20–27%. Upon light adaptation, when the pupil mechanism is activated, photoreceptor absorption decreases; in the housefly, *Musca*, by up to 6-fold. The fully light-adapted pupil diminishes the photoreceptor's acceptance angle by a factor of ~0.6 due to selective absorption of higher order waveguide modes. Spatial acuity of dark-adapted photoreceptors is more or less constant throughout the

visual wavelength range, including the UV, because the waveguide optics of the rhabdomere compromise acuity least at wavelengths most limited by diffraction of the facet lens. Diffraction is not the general limiting factor causative for UV sensitivity of insect eyes. Visual acuity is governed by diffraction only with a fully light-adapted pupil, which absorbs higher waveguide modes. Closure of the blue-absorbing pupil causes a UV-peaking spectral sensitivity of fly photoreceptors. The sensitizing pigment does not play an appreciable role in modifying spatial acuity, neither in the dark- nor the light-adapted state, due to the dominant contribution of green light in natural light sources.

Key words: rhabdomere, waveguide mode, acceptance angle, sky light, diffraction, light adaptation.

Introduction

The task of a visual system is to gain maximal optical information from the environment so that the animal can respond rapidly and appropriately to changing conditions. The eyes of higher animals therefore employ lenses, which focus light into optical waveguides harbouring the light-absorbing visual pigments. The compound eyes of flies have several hundreds to thousands of facet lenses, each focusing light from a narrow visual field into the rhabdomeres of six peripheral photoreceptors (R1–R6) and two central photoreceptors (R7 and R8). Phototransduction, the first step in vision, starts when the visual pigment in the rhabdomeres absorbs incident light (reviewed by Hardie, 2001).

Fly visual pigments utilize a special chromophore, 3-hydroxyretinal (Vogt and Kirschfeld, 1983). Connected to the opsin of the R1–R6 photoreceptors, it yields a main absorption band in the blue-green and a minor absorption band in the ultraviolet (UV). R1–R6 rhodopsin can bind the alcohol 3-hydroxyretinol, which then functions as a sensitizing pigment. The sensitizing pigment absorbs UV light and, when bound to the rhodopsin, efficiently transfers the absorbed energy to the visual pigment chromophore (Kirschfeld et al., 1977). The absorption spectrum of the sensitizing pigment–rhodopsin

complex consequently exhibits two main bands, with more or less equally high peaks in the UV and blue-green wavelength region. This characteristic underlies the typical broad-band, double-peaked sensitivity spectrum of fly R1–R6 photoreceptors (Stark et al., 1977; Kirschfeld et al., 1983).

The absorption boost in the UV is assumed to substantially improve visual performance. However, the signal increase may be minor, because the photon content of natural patterns in the UV is small compared with that of the dominant longer wavelengths, especially the green region. The question of whether the sensitizing pigment is really an advantage for fly photoreceptors is especially relevant considering the presence of the pupil mechanism. Activated by bright light, the set of pigment granules in a photoreceptor substantially reduces the light flux in the rhabdomere (Kirschfeld and Franceschini, 1969; Roebroek and Stavenga, 1990).

Electrophysiological experiments on fly photoreceptors have shown that light adaptation changes both the angular and the spectral sensitivity. It narrows the angular sensitivity for short wavelength light and increases the spectral sensitivity in the UV with respect to the sensitivity in the blue-green. Both effects were attributed to the pupil mechanism, and this has

been underscored by quantitative modelling (Hardie, 1979; Vogt et al., 1982; Smakman et al., 1984). The experiments and calculations were performed with monochromatic light. Here, I investigate the consequences of the pupil mechanism under natural illumination conditions, where the light source is spectrally broadband.

In the present paper, I investigate the sensitivity gain afforded by the sensitizing pigment vs the sensitivity drop by the light-activated pupil. To assess the maximal advantage of the sensitizing pigment for vision under natural conditions, a light source with a high UV-visible photon ratio is used, i.e. a very blue sky. It thus emerges that the sensitizing pigment noticeably raises the absolute sensitivity of a dark-adapted photoreceptor, but light adaptation of the pupil rapidly overrules this sensitivity increase. Pupil closure narrows the angular sensitivity function, which improves spatial acuity. The effect of the sensitizing pigment on the angular sensitivity is negligible.

It is often assumed that insect eyes are constrained by diffraction, because of the small size of the facet lenses, and that UV rhodopsins, first discovered in insects, are used to push the diffraction limit. However, the spatial resolution of a photoreceptor is determined by the optics of both the dioptrical system and the visual waveguide that contains the visual pigment: the facet lens and rhabdomere in the case of flies. The present analysis shows that, generally, waveguide optics compromises acuity least at wavelengths most limited by diffraction, and diffraction gets the upper hand only in the light-adapted state.

Materials and methods

Sky light radiance spectrum

The light source with a high UV-visible photon ratio is a patch of clear sky measured (on 5 June 1997) with an Oriel Instaspec I spectrophotometer equipped with a fibre of acceptance angle ($\Delta\rho$) of 7.1° ; a calibrated light source served as a reference, yielding Fig. 1. The peak radiance, 10^6 photons $s^{-1} \mu m^{-2} sr^{-1} nm^{-1}$, approximates previously measured radiance values (see McFarland and Munz, 1975; Menzel, 1979).

Visual pigment spectra

The sensitivity spectrum of fly photoreceptors depends on the diet (Stark et al., 1977). In vitamin A-deprived flies, the main sensitivity band is in the blue-green, with a peak at ~ 490 nm, and a minor band exists in the UV. The sensitivity spectrum resembles the absorption spectrum of a rhodopsin (Fig. 2, R), as given by template formulae (Stavenga et al., 2000). Feeding a vitamin A-poor fly with retinoids causes a rapid increase in UV sensitivity. The sensitivity spectrum progressively features a fine structure, characteristic of the binding of sensitizing pigment to rhodopsin molecules. In well-fed flies, the UV peak can be distinctly higher than that in the blue-green, possibly indicating binding of more than one sensitizing pigment molecule per rhodopsin (Hamdorf et al.,

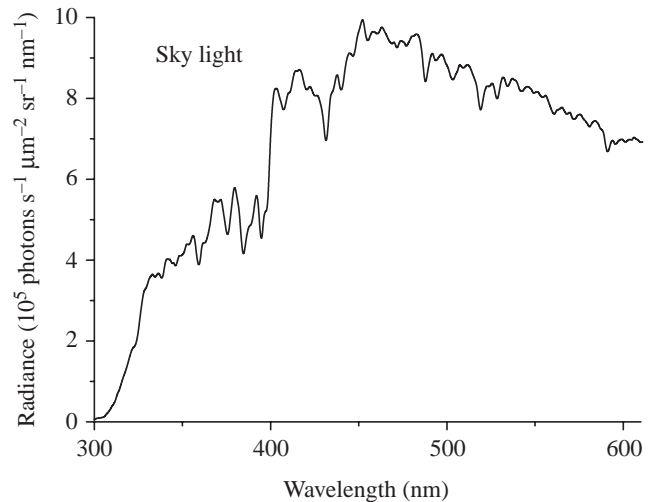


Fig. 1. Typical radiance spectrum of a UV-rich sky. The radiance in the short-wavelength range is considerably higher than that in a normal daylight spectrum.

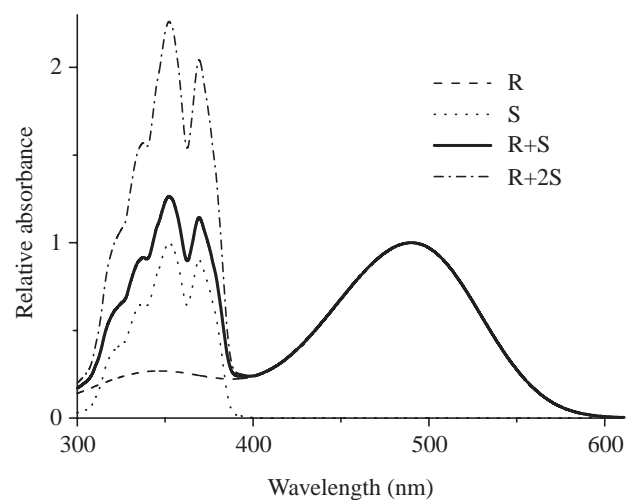


Fig. 2. Absorbance spectra of visual pigment of fly photoreceptors R1-R6. The rhodopsin, R, is sensitized by the sensitizing pigment, S. R+S and R+2S represent the cases when the rhodopsin molecule binds one and two molecules of sensitizing pigment, respectively. It is assumed that the spectra can be summed algebraically.

1992). Fig. 2 assumes that the peak value of the molecular absorbance coefficient of the sensitizing pigment (S) is identical to that of the rhodopsin (R) and that the spectra can be algebraically added when one (R+S) or two (R+2S) sensitizing pigment molecules are bound per rhodopsin.

Integrated optics of the fly facet lens-rhabdomere system

Light absorption by the visual pigment molecules of a fly photoreceptor can be calculated with the recently developed model for the fly's facet lens-rhabdomere optics (Stavenga, 2003a,b, 2004). The model is briefly as follows. Light emitted by a distant point source that enters the facet lens causes a

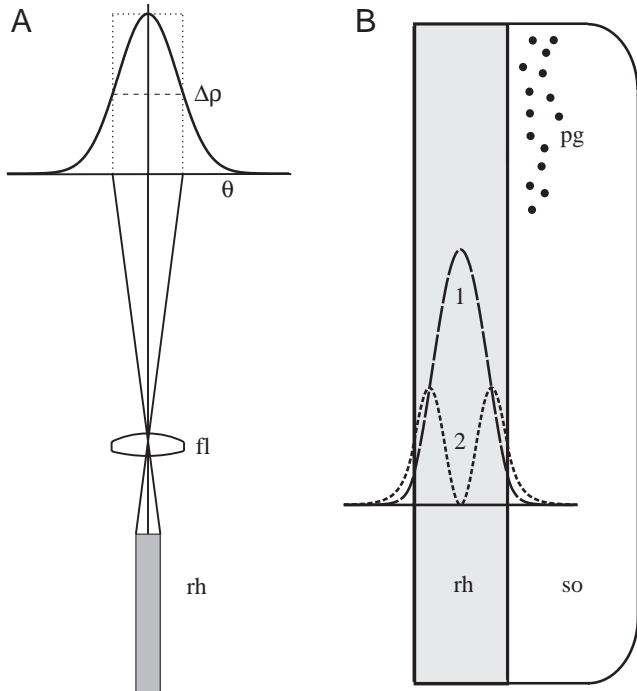


Fig. 3. Diagrams of the optics of the fly facet lens and photoreceptor rhabdomere. (A) According to geometric optics, the size of the visual field is given by the spatial angle taken up by the rhabdomere (rh) tip. Due to diffraction at the facet lens (fl) and the waveguide optics of the rhabdomere, a Gaussian-shaped angular sensitivity results with halfwidth $\Delta\rho$, the acceptance angle; θ is the incident light angle. (B) When the pigment granules (pg) in the photoreceptor soma (so) are near the rhabdomere, they absorb light from the boundary waves of the waveguide modes and thus function as a light-controlling pupil mechanism. The first mode (1) extends less far outside the rhabdomere than the second mode (2).

classical Airy-diffraction pattern in the focal plane, where the tip of the rhabdomere is located (Fig. 3A). The diameter of the facet lens and the F -number were taken to be $D_l=25\ \mu\text{m}$ and $F=2.2$, respectively (the F -number is the ratio of focal distance and lens diameter; see Stavenga et al., 1990). Part of the incident light enters the rhabdomere, where it propagates in specific waveguide patterns, so-called modes (Fig. 3B). Whether a mode is allowed or not depends on the value of the V -number: $V=\pi D_r \sqrt{n_1^2 - n_2^2} / \lambda$, where D_r is the rhabdomere diameter, n_1 and n_2 are the refractive indices of the rhabdomere interior and surrounding medium, respectively, and λ is the light wavelength. The mode with number $p=1$ is allowed for $V < 2.405$, mode $p=2$ is allowed for $V < 3.832$, mode $p=3$ for $V < 3.847$, etc. (Stavenga, 2003a). The visual pigment in the rhabdomere absorbs light from the individual modes proportionally to the absorbance coefficient of the rhabdomere medium and the fraction of the mode that exists within the rhabdomere boundary. This fraction increases with V but decreases with increasing p . Fly rhabdomeres taper and their distal tip diameter is somewhat variable (Boschek, 1971). Therefore, four distal rhabdomere diameters were explored in the calculations: $D_r=1.4, 1.6, 1.8$ and $2.0\ \mu\text{m}$. All rhabdomeres

were assumed to taper parabolically to a proximal value of $1.0\ \mu\text{m}$, whilst their length was $250\ \mu\text{m}$. The refractive index values of rhabdomere interior and surrounding medium were $n_1=1.363$ and $n_2=1.340$, respectively. The absorbance coefficient of the rhodopsin at its peak wavelength, $\lambda_{\text{max}}=490\ \text{nm}$, was set at $\alpha_{490}=0.006\ \mu\text{m}^{-1}$ (Stavenga, 2003b, 2004). The total amount of light absorbed by the visual pigment from the different modes determines the light sensitivity of the photoreceptor. The light sensitivity to a point source measured as a function of incident angle yields the angular sensitivity. This function usually approximates a Gaussian, and its halfwidth is called the acceptance angle, $\Delta\rho$ (Fig. 3a). The light sensitivity measured as a function of wavelength yields the spectral sensitivity. The angular sensitivity slightly depends on wavelength, and the spectral sensitivity slightly depends on the angle of light incidence (Stavenga, 2004).

The pupil mechanism

Fly R1–R6 photoreceptors contain small pigment granules that together enact a light-control or pupil function (Fig. 3B). The pigment granules are remotely located from the rhabdomere in the dark but, upon illumination with bright light, they migrate towards the rhabdomere. There they absorb light from the boundary wave of the modes propagating in the rhabdomere, thus reducing the light available for the visual pigment. Modes with increasing p -number have boundary waves extending further outside the waveguide boundary, and the pupil therefore progressively absorbs light from modes with increasing p . The effect of the pupil mechanism on the light flux in the rhabdomere was modelled with the same assumptions as used before (Stavenga, 2004), i.e. the pupil was fully concentrated in the most distal part of the photoreceptor, in line with experimental evidence (Roebroek and Stavenga, 1990); the pupil granules were homogeneously distributed outside a cylinder with radius $(D_r/2)+h$, where pupil distance (h)=0, 0.2, 0.4, 0.6, 0.8, $1.0\ \mu\text{m}$ and ∞ (see Fig. 4A, inset); and for the absorption spectrum of the pigment in the pupil granules the spectrum measured by Vogt et al. (1982) was used. The reduction in light flux resulting in various states of pupil closure was calculated as before (for details, see Stavenga, 2004).

A spectrally broadband and spatially extended light source, such as the blue sky of Fig. 1, usually illuminates a fly photoreceptor. The amount of light absorbed by the visual pigment in the rhabdomere then follows from the wavelength and space integral of the function that describes the light absorption from a monochromatic point source as a function of angle of incidence. The first step to determine the light sensitivity of a fly photoreceptor for sky light is therefore the derivation of the angular and spectral sensitivities.

Results

Angular sensitivity of fly photoreceptors R1–R6

Angular sensitivity functions were calculated for a facet

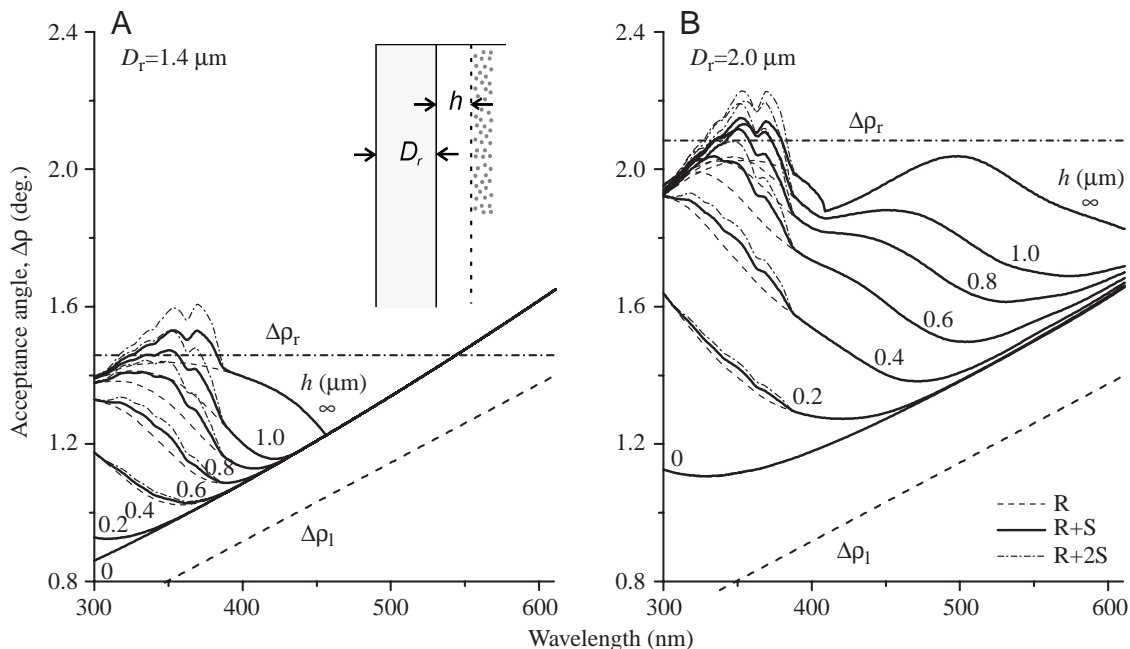


Fig. 4. Acceptance angle ($\Delta\rho$) of fly photoreceptors as a function of wavelength for different states of adaptation of the pupil. (A) Distal rhabdomere diameter $D_r=1.4\ \mu\text{m}$; (B) $D_r=2.0\ \mu\text{m}$. The rhabdomere tip is assumed to be localized in the focal plane of a $25\ \mu\text{m}$ facet lens with $F=2.2$. The rhabdomere, length $250\ \mu\text{m}$, tapers parabolic to a proximal value of $1.0\ \mu\text{m}$. The $\Delta\rho$ increases slightly in the UV with increasing sensitizing pigment. The numbers near the curves indicate the distance, h (see inset), of the front line of pupil granules to the rhabdomere border. With the pupil in the fully dark-adapted state ($h=\infty$), $\Delta\rho$ approximates $\Delta\rho_r$, the acceptance angle predicted by geometric optics. In the fully light-adapted state, given by $h=0\ \mu\text{m}$, where the higher modes are completely suppressed, $\Delta\rho$ approaches $\Delta\rho_1$, the halfwidth of the angular diffraction function. The angular sensitivity is broadened due to the non-negligible diameter of the rhabdomere.

lens with diameter $D_l=25\ \mu\text{m}$ and $F=2.2$, for four rhabdomeres with distal diameter $D_r=1.4, 1.6, 1.8$ and $2.0\ \mu\text{m}$, all tapering over a distance of $250\ \mu\text{m}$ to a proximal diameter of $1.0\ \mu\text{m}$, for three different visual pigment complexes (R, R+S and R+2S; Fig. 2) and for wavelengths 300–610 nm. Fitting the angular sensitivity curves calculated at each wavelength with a Gaussian function yielded the acceptance angle as a function of wavelength, $\Delta\rho(\lambda)$. Fig. 4A presents the results for a distal rhabdomere diameter $D_r=1.4\ \mu\text{m}$, and Fig. 4B shows those for $D_r=2.0\ \mu\text{m}$. The angular sensitivity functions were also calculated for seven different states of the pupillary pigment.

When $D_r=1.4\ \mu\text{m}$ (Fig. 4A), only one waveguide mode is allowed for $\lambda>456\ \text{nm}$, the cut-off wavelength of the second mode. For wavelengths above $456\ \text{nm}$, pupil absorption diminishes the absolute sensitivity, but this does not affect the acceptance angle because only one mode exists. The situation changes for $\lambda<456\ \text{nm}$, because the two modes that can then exist have different boundary waves. With increasing pupil closure (i.e. with decreasing h ; see Fig. 4A, inset), the pupil absorbs progressively more strongly from the second mode than from the first mode. This means that the second mode vanishes and the first mode increasingly determines the value of $\Delta\rho$. In the process of pupil closure, $\Delta\rho$ therefore first decreases for blue light, near $\lambda\approx 450\ \text{nm}$. Later on, $\Delta\rho$ also diminishes in the UV (Fig. 4A).

When $D_r=2.0\ \mu\text{m}$ (Fig. 4B), the cut-off wavelengths of the second, third, fourth and fifth modes are $651, 409, 407$ and $305\ \text{nm}$, respectively. Upon pupil closure, $\Delta\rho$ decreases initially most prominently at wavelengths between 400 and $650\ \text{nm}$, again because of the dominant contribution of the second mode to the angular sensitivity. With progressing pupil closure, $\Delta\rho$ finally also falls in the UV (Fig. 4B).

The $\Delta\rho$ following from geometric optics for a rhabdomere with distal diameter D_r is given by $\Delta\rho_r=D_r/f=D_r D_l/F$, where f is the facet lens' focal distance. With $D_l=25\ \mu\text{m}$ and $F=2.2$, the diameters $D_r=1.4$ and $2.0\ \mu\text{m}$ yield $\Delta\rho_r=1.46^\circ$ and 2.08° , respectively (Fig. 4). The $\Delta\rho$ values calculated with the wave-optics model for dark-adapted photoreceptors depend on wavelength but fluctuate around the geometric value. $\Delta\rho_0(\lambda)$, the acceptance angle in the maximally light-adapted state ($h=0\ \mu\text{m}$), runs approximately parallel to $\Delta\rho_1(\lambda)=\lambda/D_l$ for both diameter values (Fig. 4). $\Delta\rho_1$ is the halfwidth of an Airy-diffraction curve, which would be the $\Delta\rho$ of a point detector, i.e. a photoreceptor with a rhabdomere of negligible diameter (Snyder, 1979). A non-negligible rhabdomere diameter broadens the acceptance angle by a factor, $\Delta\rho_0/\Delta\rho_1$, that is similar for both $D_r=1.4$ and $2.0\ \mu\text{m}$: 1.19 and 1.20 ; average over the wavelength range 450 – $600\ \text{nm}$ (see van Hateren, 1984; Stavenga, 2004).

The acceptance angles in the UV wavelength range slightly increase with an increase in the amount of sensitizing pigment.

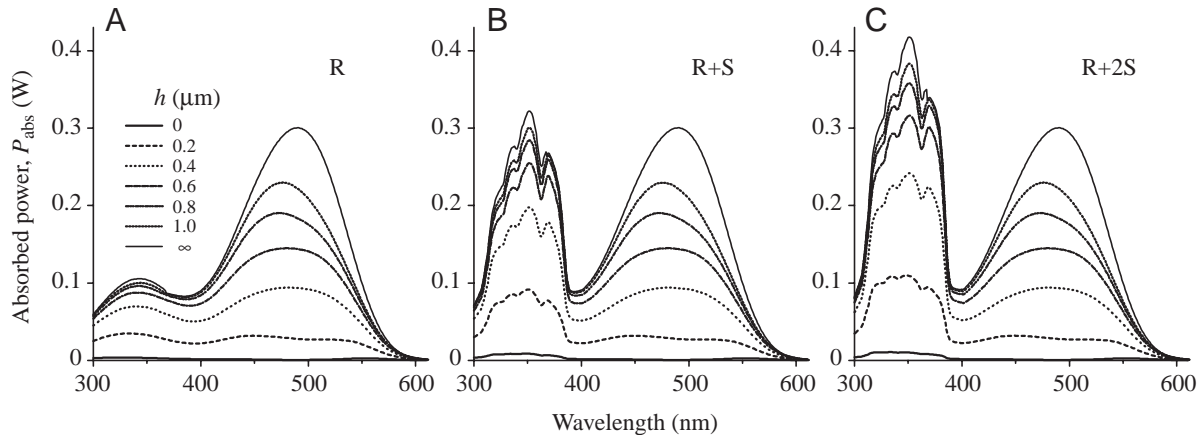


Fig. 5. Absorption spectra for different states of light adaptation, given by the pupil distance, h (Fig. 4A, inset). At all wavelengths, a uniform light source with radiance $1 \text{ W sr}^{-1} \mu\text{m}^{-2}$ illuminates a $25 \mu\text{m}$ facet lens ($F=2.2$) with, in its focal plane, the distal end of a rhabdomere with diameter $2.0 \mu\text{m}$. (A) Pure rhodopsin (R). Pupil closure causes an overall reduced absorption spectrum. (B) One sensitizing pigment molecule per rhodopsin (R+S). A distinct UV peak remains upon pupil closure. (C) Two sensitizing pigment molecules per rhodopsin (R+2S). The UV peak is only slightly higher than that in B due to self-screening.

The effect of the sensitizing pigment on $\Delta\rho$ diminishes when the pupil closes (Fig. 4).

Spectral sensitivity of fly photoreceptors R1–R6

The sensitivity spectrum of a photoreceptor is similar to the absorption spectrum of the visual pigment when spectrally selective filtering pigments are absent. Minor spectral modifications result from self-screening, the effect of diminishing contribution to absorption by visual pigment located increasingly proximally in the rhabdomere. More important modulations are caused by waveguide effects, because the excitation of waveguide modes strongly depends on both the angle of incidence and wavelength of the light source (Fig. 4).

Integration of the light absorption over the angle of incidence at all wavelengths yields the absorption spectrum with an extended light source. Fig. 5 presents the absorption spectra of a photoreceptor illuminated by a spatially uniform, monochromatic light source, the wavelength of which varied from 300 to 610 nm, with a radiance of $1 \text{ W sr}^{-1} \mu\text{m}^{-2}$. The rhabdomere had a distal diameter $D_r=2.0 \mu\text{m}$, tapering to $1.0 \mu\text{m}$, and length $250 \mu\text{m}$ and contained visual pigment with a peak absorbance coefficient of the rhodopsin of $\alpha_{490}=0.006 \mu\text{m}^{-1}$. One or two sensitizing pigment molecules per rhodopsin were added (see Fig. 2 and Materials and methods).

Fig. 5 shows that the absorption spectra resulting for fly rhodopsin without sensitizing pigment (Fig. 5A), with one (Fig. 5B) and with two (Fig. 5C) sensitizing pigment molecules per rhodopsin resemble the absorbance spectra of the visual pigment complexes (Fig. 2) when the pupil pigment granules are remote from the rhabdomere ($h=\infty$). The absorption band in the UV of Fig. 5C has a somewhat depressed relative height compared with the UV band of the visual pigment's molecular absorbance spectrum (Fig. 2), due to self-screening. Pupil

closure results in reduced light absorption by the visual pigment at all wavelengths. This occurs due to reduction of the light power propagating in the second mode, predominantly in the blue-green wavelength range. When pupil activation is moderate, the absorbance band in the blue-green shifts towards the blue. The pupil increasingly filters the higher order modes in the UV, but the contribution of these modes to the light power absorbed by the visual pigment is relatively minor. The outcome is thus that the closing pupil predominantly suppresses the blue-green band of the visual pigment's absorbance spectrum and much less affects the UV peak. The same calculations performed for rhabdomeres with smaller diameters give very similar results. Light-adapted photoreceptors with no sensitizing pigment obtain a more or less flat absorption spectrum, but with sensitizing pigment, pupil closure produces spectra with a clear UV peak.

Intracellular recordings of fly photoreceptors in different light-adapted states showed a shifted blue-green peak and a change in relative height of the blue-green vs UV band, resembling the spectra of Fig. 5 (Hardie, 1979; Vogt et al., 1982). The hypothesis that a short-wavelength-filtering pupil caused these effects is now substantiated in reasonably quantitative detail (see also Stavenga, 2004).

Absolute light sensitivity of a fly photoreceptor for sky light

The pupil-induced prominent UV band (Fig. 5), i.e. an increased UV sensitivity relative to the sensitivity in the blue-green, might suggest that the function of the sensitizing pigment is to enhance light absorption from natural, UV-rich patterns. This hypothesis can be tested by calculating the light absorption from the sky, because this natural light source has a prominent band in the UV. The amount of absorbed light is obtained by integration of the sky radiance (Fig. 1) multiplied by the (absolute) sensitivity for an extended light source (Fig. 5) over the wavelength range of the photoreceptor's

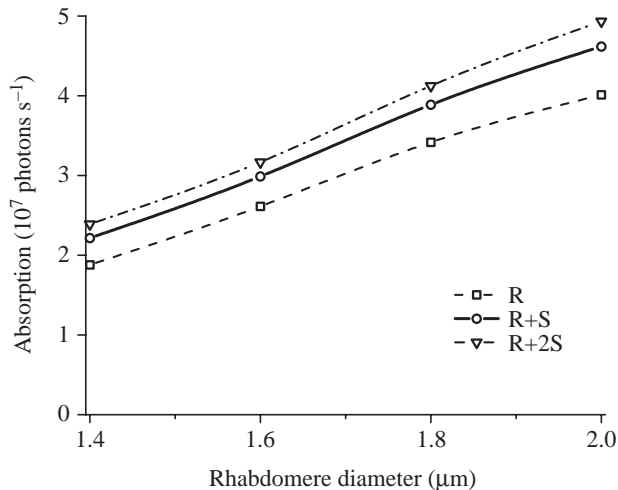


Fig. 6. Absorbed number of photons per second by a photoreceptor, with pure rhodopsin (R) and with one (R+S) or two (R+2S) sensitizing pigment molecules per rhodopsin, from a sky with radiance given by Fig. 1, for a fully dark-adapted photoreceptor ($h=\infty$; see Fig. 4A, inset), as a function of distal rhabdomere diameter. Photon absorption increases with rhabdomere diameter. One sensitizing pigment molecule per rhodopsin increases the absorption by 14–18% with respect to pure rhodopsin, and two sensitizing pigment molecules per rhodopsin increase the absorption by 20–27%.

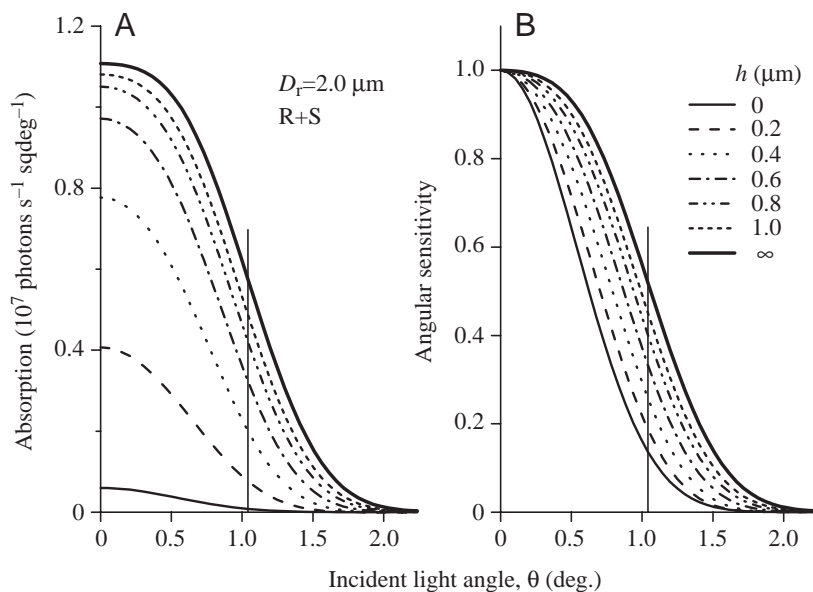


Fig. 7. The absorption of sky light as a function of the angle of the incident light for different states of pupil closure for a photoreceptor with a distal rhabdomere diameter of 2 μm and one sensitizing pigment molecule per rhodopsin (R+S). The pupil adaptation is given by the pupil distance, h . (A) Photon absorption per second from a patch of blue sky of 1 square degree seen under an angle θ . (B) Normalization shows that the angular sensitivity function distinctly narrows upon light adaptation. The vertical lines indicate the angle of incident light that is focused on the rhabdomere border.

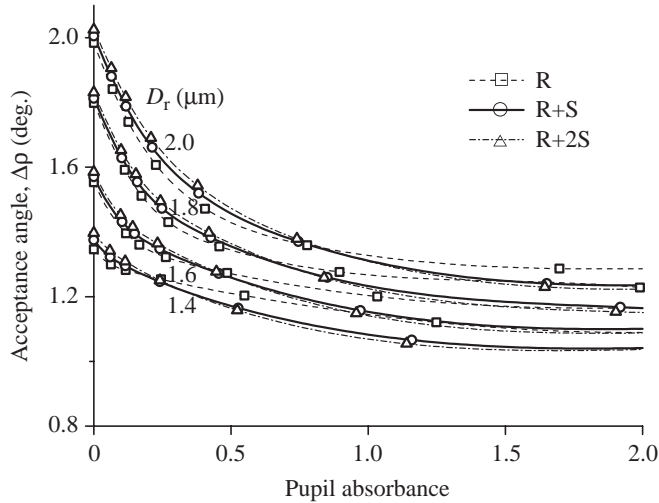
spectral sensitivity. Fig. 6 presents the total photon absorption as a function of rhabdomere diameter (all with the facet lens of diameter $D_1=25\ \mu\text{m}$ and $F=2.2$) for a dark-adapted photoreceptor. One sensitizing pigment molecule per rhodopsin increases the photoreceptor absorption by 14–18% with respect to pure rhodopsin, whilst two sensitizing pigment molecules per rhodopsin increase the absorption by 20–27%, depending on the distal rhabdomere diameter (Fig. 6). The wavelength integrals of the visual pigment spectra of Fig. 2 reveal that one or two sensitizing pigment molecules per rhodopsin increase the molecular absorbance coefficient by 38% or 76%, respectively. These numbers are much larger than those for the integral photon absorptions. This is due firstly to self-screening and secondly to the modest number of UV vs blue-green photons, even in the UV-rich sky. Of course, the light-capture increase by the sensitizing pigment vanishes for light sources that emit few UV photons, such as natural light reflected from green plants.

Angular sensitivity changes due to a closing pupil

Fig. 6 shows that the sensitizing pigment enhances light sensitivity under light conditions where the pupil is not activated, but pupil closure rapidly erases the gain in light absorption. Since the pupil also causes a decrease in $\Delta\rho$, we can speculate that the sensitizing pigment has a special beneficial effect on the improved spatial acuity in natural conditions. This possibility can be investigated by calculating the angular sensitivity for sky light. Fig. 7 presents the light absorption in photons per second by a 2.0 μm rhabdomere, containing a visual pigment with one sensitizing pigment molecule per rhodopsin, from a patch of sky (Fig. 1) measuring 1 square degree (3.05×10^{-4} sr) seen at various angles. Pupil closure reduces the absolute absorption (Fig. 7A), and normalization shows that it narrows the angular sensitivity curve (Fig. 7B). The shapes of the angular sensitivity curves are well approximated by Gaussians.

Pupil absorbance and photoreceptor acceptance angle

Fig. 8 presents the $\Delta\rho$ values resulting from Gaussian fits to the angular sensitivity curves for the four rhabdomere diameters (Fig. 6), combined with the three visual pigment complexes and the seven states of the pupil (Fig. 5), plotted as a function of pupil absorbance. The pupil absorbance was calculated as follows (see Stavenga, 2004). First, the total photon absorption by the visual pigment, $P_{\text{abs}}(h)$, from an extended, uniform sky (Fig. 1) was calculated for the various states of the pupil, given by pupil distance h . Of course, $P_{\text{abs}}(\infty)$, the photon absorption in the dark-adapted state, is maximal. The absorption reduces to $P_{\text{abs}}(h)$ when the pupil closes or, equivalently, its transmittance decreases from its maximal value



$T(\infty)=1$ to $T(h)=P_{\text{abs}}(h)/P_{\text{abs}}(\infty)$. The pupil absorbance then follows from the definition: $A(h)=-\log_{10}T(h)$; $A(\infty)=0$ corresponds to the dark-adapted state (Fig. 8). The $\Delta\rho(A)$ curves for the three different visual pigment cases (R, R+S, R+2S) at a given D_r are very similar at pupil absorbances below 0.7, which suggests that the sensitizing pigment then has virtually no effect on the spatial acuity. Extreme pupil closure and sensitizing pigment content lowers the acceptance angle by a few percent.

Fig. 8 shows that an increase in pupil absorbance is accompanied by a decrease in $\Delta\rho$ for all rhabdomere values. The decrease stabilizes for pupil absorbances above ~ 1.5 . The question can now be asked: are these high absorbance values actually attained in fly photoreceptors under natural conditions? An answer can be obtained from electrophysiological and optical experiments.

Illumination of a photoreceptor with a step of light depolarizes the cell membrane, which rapidly reaches a peak and then levels off to a plateau (Hardie, 1985). Fig. 9A reproduces peak and plateau potential values derived from intracellular recordings of a *Musca* photoreceptor (Vogt et al., 1982). The data are plotted together with the ratio of the sensitivity for test flashes of 500 and 359 nm light, S_{500}/S_{359} , as a function of the log intensity of the applied orange adapting light. The measured sensitivity ratio was ~ 1 in the dark-adapted state, approximating the case of Fig. 5B, where the visual pigment has one sensitizing pigment molecule per rhodopsin. Fig. 9A shows that the sensitivity ratio gradually dropped when the intensity of the adapting light increased by several log units. The adapting light apparently activated the pupil, which caused a decrease in the ratio S_{500}/S_{359} , settling at ~ 0.35 in the fully light-adapted state (Fig. 9A).

The principal result of pupil closure is a decrease in light flux, and therefore the decrease in the ratio S_{500}/S_{359} is intimately connected to the pupil absorbance. The connection can be determined by assuming that the sensitivity ratio is equivalent to the ratio of the absorption of 500 and 359 nm light. Calculations of the absorption ratio together with the

Fig. 8. Acceptance angle vs pupil absorbance calculated for three visual pigment conditions, pure rhodopsin (R), one (R+S) and two (R+2S) sensitizing pigment molecules per rhodopsin, for photoreceptors with distal rhabdomere diameters 1.4–2.0 μm . For each of the seven pupil states the acceptance angle as well as the total absorption of a uniformly radiating sky were calculated. The pupil absorbance was obtained by taking minus the decadic logarithm of the absorption relative to that for the dark-adapted state ($h=\infty$; the case of Fig. 6).

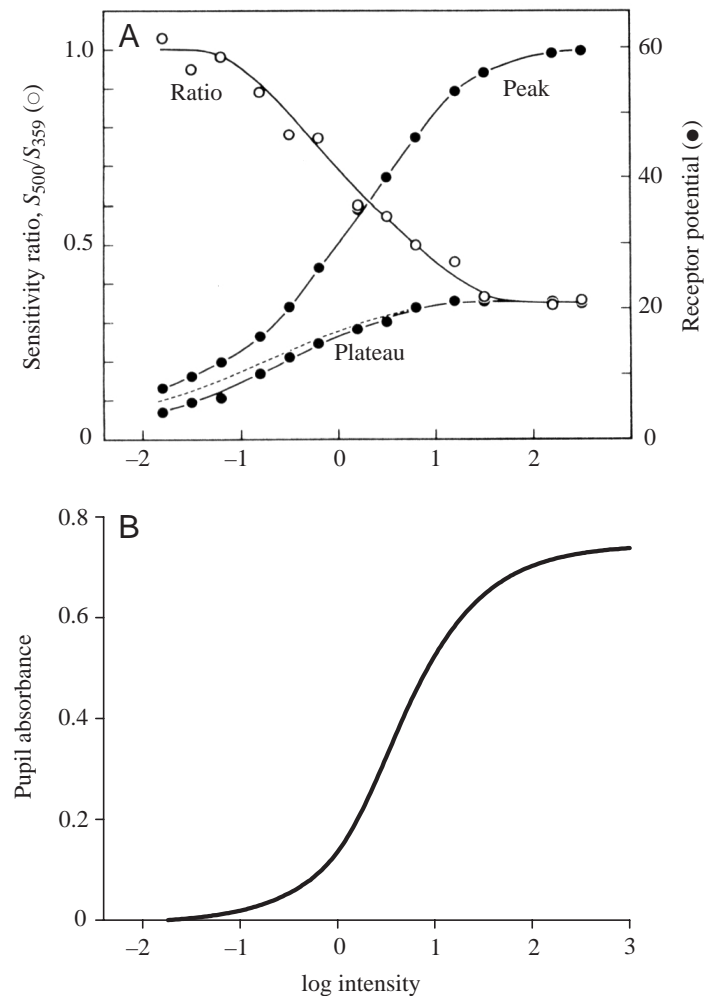


Fig. 9. (A) Ratio between the sensitivity for 500 nm and 359 nm light determined from intracellular, electrophysiological recordings of a *Musca* photoreceptor adapted to orange light, the intensity of which is indicated in decadic log units (abscissa; from Vogt et al., 1982). The peak and plateau potential (dotted line, 30 s light adaptation; continuous line, 150 s adaptation) indicate the sensitivity range of the photoreceptor. (B) Pupil absorbance as a function of log adaptation intensity derived from the sensitivity ratio of A together with the relationship between the average sensitivity ratio and the pupil absorbance for photoreceptors with one sensitizing pigment molecule per rhodopsin (Fig. 10, av).

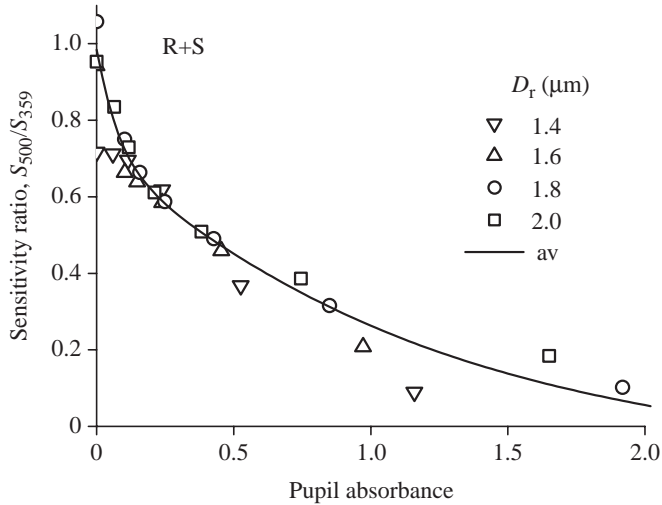


Fig. 10. Ratio between the sensitivity for 500 nm and 359 nm light of photoreceptors with distal rhabdomere diameters of 1.4–2.0 μm and one sensitizing pigment molecule per rhodopsin (R+S), obtained by calculating the relative absorption of 500 nm and 359 nm light at the various pupil states (given in Fig. 4), plotted vs the pupil absorbance for sky light at the same pupil state, together with a spline fit (av). The sensitivity ratio decreases due to selective suppression of the absorption in the blue-green wavelength range by the pupil.

pupil absorbance for all rhabdomere radii and pupil states (given by parameter h), and taking one sensitizing pigment molecule per rhodopsin, yielded the data points of Fig. 10. The data points are reasonably well approximated by a single, average curve (Fig. 10, av). With this curve, the sensitivity ratio–log intensity function of Fig. 9A can be translated into a pupil absorbance–log intensity function. The result (Fig. 9B) indicates that the saturated pupil in the *Musca* photoreceptor of Vogt et al. (1982) would reduce the effective flux of sky light by almost 0.8 log units, i.e. by a factor of ~ 6 . A pupil absorbance of 0.8, corresponding to about $h=0.2$, reduces the $\Delta\rho$ to near its minimal value (Figs 7, 8). Pupil absorbance and $\Delta\rho$ reduction may be less under natural sky light, because fly photoreceptors will not be fully saturated (Anderson and Laughlin, 2000).

Discussion

The model applied here for studying the effect of the sensitizing pigment and the pupil on the visual performance of fly photoreceptors rests on several assumptions. First, concerning the anatomy, the facet lenses are assumed to be ideal, i.e. aberration free and only diffraction limited. This is probably a valid approximation, because the facet lens is only about 50 times the wavelength of light, and diffraction then dominates the imaging properties of a lens. The rhabdomere is assumed to have its tip in the focal plane of the facet lens. This is certainly not true for all wavelengths due to the unavoidable dispersion of the facet lens' refractive index, but model calculations show that the optics of the facet lens–rhabdomere

system is quite robust to defocus (Stavenga, 2003a,b). The assumption that the rhabdomere is a circular cylinder is only very approximately true, as its cross-section is often a distorted ellipse. Although the waveguide modes then are different from those in a circular cylinder, the absorption of light by the visual pigment is presumably similar. The assumption that the rhabdomere tapers from distal to proximal in a parabolic fashion is based on the anatomy of *Musca* (Boschek, 1971). Anatomical data from other flies suggest that tapering is a universal characteristic of R1–R6 photoreceptors. Although the precise shape is generally unknown, model calculations with linear vs parabolic tapering show minor differences in the absorbed light power.

The absorption spectrum of the visual pigment of fly photoreceptors is modelled with a vitamin A1-based rhodopsin template. The rhodopsin of flies is based on vitamin A3 (Kirschfeld, 1986), but its absorption spectrum probably follows the same rules as that of vitamin A1 rhodopsins (Stavenga et al., 1993). The simple algebraic addition of a sensitizing pigment is most likely an oversimplification, but exact absorption spectra of visual pigment plus sensitizing pigment are not known, and the modelling results are probably insensitive to it.

Concerning the pupil, it is assumed to exert its light-controlling action at the extreme distal end of the photoreceptor, as if it in fact functions as a light filter in front of the visual pigment. The pupil pigment granules are distributed in the photoreceptor soma (Boschek, 1971), but experimental data strongly argue in favour of a distal pupil (Roebroek and Stavenga, 1990). What counts for a photoreceptor is not the number of absorbed photons converting rhodopsin molecules but the change in membrane potential created and the signal transmitted by the photoreceptor synapse. Under bright light conditions, the distal end of the photoreceptor is strongly light adapted and consequently more desensitized than the proximal elements of the photoreceptor's phototransduction machinery. The part of the photoreceptor proximal to the pupil will then determine the photoreceptor's performance. The rhabdomeres of R1–R6 photoreceptors taper, so that an extreme gradient in longitudinal adaptation causes a relatively stronger contribution of the proximal part of the photoreceptor's phototransduction machinery. As we do not know whether or not the molecular composition of the microvilli varies along the photoreceptor length, adaptation effects are difficult to assess.

The absorption spectrum of the pupil granules used in the modelling was measured in squash preparations (Vogt et al., 1982), making the precise shape of the spectrum slightly uncertain, but this will have no major effects on the calculated results. The density of the granules is another uncertainty, but the concentration was chosen so that measured absorbances could be accommodated by the model (see Stavenga, 2004). Furthermore, the distribution of the pupillary granules was assumed to be homogeneous outside a cylinder with radius $(D_r/2)+h$ that surrounds the rhabdomere. The soma of a fly

photoreceptor in fact occupies only a small sector, and thus the pupil can only affect a restricted part of the boundary wave. Presumably, however, the absorbances of pupils fully and partially surrounding the rhabdomere are proportional.

Only waveguide modes propagating bound to the rhabdomere have been taken into account. Unbound modes travel along the rhabdomere for a limited distance and lose their light power by radiation. The light absorption from unbound modes broadens the angular sensitivity curves, thus reducing the wavelength dependence of $\Delta\rho$, i.e. the spectra of Fig. 4 become flatter, especially those below or near pupil threshold. Also, the unbound modes will have a smoothing effect on the spectral sensitivity near the cut-off wavelengths.

Notwithstanding all assumptions and approximations, the modelling provides considerable insight into the consequences of the sensitizing pigment and the actions of the pupil. The model calculations show that the UV-absorbing sensitizing pigment of fly R1–R6 photoreceptors boosts the sensitivity for UV-rich skylight by 14–27%, depending on the size of the rhabdomere and the presence of one or two sensitizing pigment molecules per rhodopsin (Fig. 6). The sensitivity increase will be less for light sources with a less prominent UV content than the sky. The conclusion thus is that the sensitizing pigment has a sizeable benefit only when the light source contains a substantial amount of UV and that its value will become rather unimpressive when UV content is minor. The employment of sensitizing pigment nevertheless is probably well worth the costs. As pointed out by Kirschfeld (1992), the mass of a sensitizing pigment molecule is less than 2% of that of a rhodopsin molecule, meaning that a sensitivity improvement of more than a few percent will already pay off.

Installing the sensitizing pigment purely for improving light sensitivity can only be of limited value, i.e. at light intensities below or near pupil threshold. This presumably holds for strongly shaded areas, but direct measurements will be necessary to substantiate this point. The few percent gain in sensitivity is rapidly lost when the pupil is activated, which occurs at intensities depolarizing the receptor by ~10 mV (Fig. 9). These intensities are easily reached in daylight (Anderson and Laughlin, 2000), in the sunlit areas where flies are often active, and most probably when males are chasing high-contrast females against the blue sky. Such bright lights substantially reduce R1–R6 $\Delta\rho$.

Pupil closure causes narrowing of the angular sensitivity function, by an extreme factor of ~0.6, somewhat depending on rhabdomere diameter and visual pigment composition (Fig. 8). The sampling of spatial frequencies thus changes appreciably, although the sampling basis, the interommatidial angle, remains constant. The narrowing of the angular sensitivity by bright light possibly counters the motion blurring that smears visual objects during high-speed aerial acrobatics in both pursuing and pursued flies (Burton and Laughlin, 2003), activities typically enjoyed in warm, bright-light conditions.

The interplay of increased sensitivity by the sensitizing pigment, being 14–27%, and the reduced sensitivity by the

pupil, necessary for improving spatial acuity, has special relevance for the so-called lovespot in the dorso-frontal area of the eyes of male flies. The central R7 and R8 photoreceptors, redesigned to supplement the sensitivity of the achromatic contrast system mediated by the R1–R6 photoreceptors (Hardie, 1985), yield a sensitivity increase of perhaps 10%. This, of course, is to the detriment of the chromatic channel normally mediated by the pair of central photoreceptors. We should note here that the pupil of R7 is probably less effective than that in R1–R6, due to the smaller soma, but the rhabdomere diameter is also smaller, yielding a smaller acceptance angle. In this way, loss in absolute sensitivity, unavoidable for achieving a small acceptance angle, is recovered by recruiting R7 to join the R1–R6 system. Large facet lenses and adjustments in the phototransduction machinery are additional factors for realizing enhanced contrast detection by photoreceptors in the male lovespot (Burton and Laughlin, 2003).

It is important to note here that the facet lens and rhabdomere waveguide together determine the total light absorption of a photoreceptor. The facet lens diameter is enlarged in areas of fly eyes with high acuity, but the *F*-number of the facet lenses remains virtually constant across the eye (Stavenga et al., 1990). The *F*-number is the only parameter of the facet lens that determines the photoreceptor absorption from an extended light source, given a certain size of the rhabdomere (Stavenga, 2003a). If the tip of the rhabdomere coincides with the focal plane of the facet lens, the size of the visual field is inversely proportional to the focal distance and, with *F* constant, also to the facet lens diameter. The larger facets of the lovespot hence cause a smaller photoreceptor receptive field. A dark object, perhaps a distant female, more readily creates a visible contrast in a small spatial field than in a wider field, and in this way males have a visual discrimination advantage over females (Burton and Laughlin, 2003). Of course, larger facets take up more space, which is lost for eye parts elsewhere. Consequently, the high acuity in the lovespot comes at the cost of lower acuity in other eye areas. But, for hunters, it is important to have exquisite eye sight in forward-looking directions, whereas chased animals must distribute their visual attention more uniformly.

Pupil closure reduces the light flux in the rhabdomere and thus expands the intensity working range of the photoreceptor (Howard et al., 1987). Using data from the housefly *Musca*, an extreme pupil absorbance of 0.8 was deduced (Fig. 9B). Much higher absorbance values, up to ~2 in saturation, were determined in electrophysiological and optical measurements on the blowfly *Calliphora* (Howard et al., 1987; Roebroek and Stavenga, 1990). A high pupil absorbance removes, or at least reduces, the difference in sensitivity between the dark-adapted R1–R6 and R7, R8 photoreceptors, estimated to be ~1.3 log units (Anderson and Laughlin, 2000). The different pupil absorbances of housefly and blowfly may indicate that the effectiveness of the pupil mechanism depends on species, which also follows from direct optical measurements on hoverflies, where the pupil transmittance dropped locally by no more than

a factor of 2, i.e. a maximal absorbance of no more than 0.3 could be measured (Stavenga, 1979). The connected change in angular sensitivity will be minor, suggesting a lifestyle with less variable light conditions, but this point needs further study.

The pupil is well able to achieve a high acuity by cutting out the higher order waveguide modes, but the case of the fly R1–R6 photoreceptors shows that acuity is not pushed to the lowest values achievable. Because diffraction increases with wavelength and broadband natural patterns always have an excessive number of long-wavelength photons, a UV rhodopsin is necessary to realize the smallest acceptance angle. The $\Delta\rho$ of fully light-adapted R1–R6 fly photoreceptors is slightly larger than would be possible with a pure UV rhodopsin, even when the blue-green peak of the rhodopsin is suppressed in favour of the sensitizing pigment (Figs 4, 8). We have to realize, however, that acuity is the result of both facet lens and waveguide optics. Acuity increases with an increasing facet lens diameter, a decreasing rhabdomere diameter and a more active pupil that removes higher order modes. Where the optimum is depends on many factors that are determined by the habitat and the animal's behavior, e.g. the intensity range where it is active, its flight velocities and sex.

In the dark-adapted state, $\Delta\rho$ is only slightly wavelength dependent and approximates the constant value following from geometrical optics, $\Delta\rho_r$ (Fig. 4). The closing pupil initially reduces $\Delta\rho$ in the middle wavelength range, where the pupil absorbs light propagated in the second mode (Fig. 4). The pupil reduces $\Delta\rho$ in the UV only when the light adaptation process approaches saturation. $\Delta\rho$ then approximates values dictated by diffraction, $\Delta\rho_r = \lambda/D_1$.

Diffraction is often assumed to be the crucial factor that limits imaging by the small facet lenses of insect eyes, and it is hence thought that insects have extended their sensitivity into the UV by developing UV-transparent lenses and UV-absorbing rhodopsins, so that optimal acuity is achieved. This notion, going back to Mallock (1894), neglects the important contribution to visual acuity by the visual waveguides, the rhabdomeres of flies and the fused rhabdoms of bees and butterflies. Fig. 4 shows that diffraction is dominant when the rhabdomere is so slender that only one mode is allowed or, in a wider rhabdomere, when the pupil has extinguished all higher order modes. Several waveguide modes are excited in a fat rhabdomere and/or at short wavelengths. The second and third mode are excited by off-axis illumination, which results in broadening of the angular sensitivity curve (Fig. 7; Stavenga, 2004). This broadening increases with visual pigment absorption (Fig. 4) and can almost fully compensate the limitations set by diffraction. This conclusion holds in principle for all eyes that employ lens–waveguide systems. The widespread opinion that insect eyes, with their small facet lenses, are more constrained by diffraction than other eyes therefore needs revision. Vision research of recent decades has sufficiently demonstrated that UV vision is by no means the prerogative of insects or invertebrates. Furthermore, the larger eyes of vertebrates also suffer from diffraction, but are

perhaps more constrained by optical errors, such as spherical and chromatic aberration.

The present model calculations indicate that the sensitizing pigment of fly eyes primarily functions for enhancing light sensitivity at low light levels and that the pupil functions to improve visual performance at high light levels by expanding the photoreceptor working range and improving spatial acuity. Its third function, namely to shift the photochemical cycle of the visual pigment, thus favouring rhodopsin photoreconversion (Stavenga, 2002), requires a separate study.

List of symbols

$\Delta\rho$	acceptance angle
$\Delta\rho(\lambda)$	acceptance angle as a function of wavelength
$\Delta\rho_r$	acceptance angle from geometric optics
$\Delta\rho_1$	acceptance angle from diffraction optics
A	pupil absorbance
D_1	diameter of facet lens
D_r	diameter of rhabdomere
f	focal distance of the facet lens
F	ratio of focal distance and lens diameter
h	pupil distance
n_1	refractive index of rhabdomere interior
n_2	refractive index of rhabdomere surrounding medium
p	mode number
P_{abs}	photon absorption by the visual pigment
T	pupil transmittance
V	waveguide number
θ	incident light angle
α	absorbance coefficient
λ	wavelength of light
λ_{max}	visual pigment absorption peak wavelength

This research was supported by the EOARD. Hein Leertouwer provided technical support. Drs Brian Burton, Roger Hardie, Simon Laughlin and Eric Warrant provided generous comments concerning the manuscript.

References

- Anderson, J. C. and Laughlin, S. B. (2000). Photoreceptor performance and the co-ordination of achromatic and chromatic inputs in the fly visual system. *Vision Res.* **40**, 13–31.
- Boschek, B. (1971). On the fine structure of the peripheral retina and lamina ganglionaris of the fly, *Musca domestica*. *Z. Zellforsch.* **118**, 369–409.
- Burton, B. G. and Laughlin, S. B. (2003). Neural images of pursuit targets in the photoreceptor arrays of male and female houseflies *Musca domestica*. *J. Exp. Biol.* **206**, 3963–3977.
- Hamdorf, K., Hochstrate, P., Höglund, G., Moser, M., Sperber, S. and Schlecht, P. (1992). Ultra-violet sensitizing pigment in blowfly photoreceptors R1–6; probable nature and binding sites. *J. Comp. Physiol. A* **171**, 601–615.
- Hardie, R. C. (1979). Electrophysiological analysis of the fly retina. I. Comparative properties of R1–6 and R7 and R8. *J. Comp. Physiol. A* **129**, 19–33.
- Hardie, R. C. (1985). Functional organization of the fly retina. In *Progress in Sensory Physiology*, vol. 5 (ed. D. Ottoson), pp 1–79. Berlin, Heidelberg, New York: Springer.
- Hardie, R. C. (2001). Phototransduction in *Drosophila melanogaster*. *J. Exp. Biol.* **204**, 3403–3409.

- Howard, J., Blakeslee, B. and Laughlin, S. B.** (1987). The intracellular pupil mechanism and photoreceptor signal:noise ratios in the fly *Lucila cuprina*. *Proc. R. Soc. Lond B* **231**, 415-435.
- Kirschfeld, K.** (1986). Activation of visual pigment: chromophore structure and function. In *The Molecular Mechanism of Photoreception* (ed. H. Stieve), pp. 31-49. Berlin, Heidelberg, New York: Springer.
- Kirschfeld, K.** (1992). Wie wird im Verlauf der Evolution optimiert? "Erfindungen" im Komplexauge der Stubenfliege. In *Technische Biologie und Bionik 1, 1. Bionik-Kongress, Wiesbaden* (ed. W. Nachtigall), pp. 39-52. Stuttgart: Gustav Fischer.
- Kirschfeld, K. and Franceschini, N.** (1969). Ein Mechanismus zur Steuerung des Lichtflusses in den Rhabdomeren des Komplexaugus von *Musca*. *Kybernetik* **6**, 13-22.
- Kirschfeld, K., Franceschini, N. and Minke, B.** (1977). Evidence for a sensitising pigment in fly photoreceptors. *Nature* **269**, 386-390.
- Kirschfeld, K., Feiler, R., Hardie, R. C., Vogt, K. and Franceschini, N.** (1983). The sensitizing pigment in fly photoreceptors. *Biophys. Struct. Mech.* **10**, 81-92.
- Mallock, A.** (1894). Insect sight and the defining power of composite eyes. *Proc. R. Soc. Lond. B* **55**, 85-90.
- McFarland, W. N. and Munz, F. W.** (1975). The photic environment of clear tropical seas during the day. *Vision Res.* **15**, 1071-1080.
- Menzel, R.** (1979). Spectral sensitivity and color vision in invertebrates. In *Handbook of Sensory Physiology*, vol. VII/6A (ed. H. Autrum), pp. 503-580. Berlin, Heidelberg, New York: Springer.
- Roebroek, J. G. H. and Stavenga, D. G.** (1990). On the effective density of the pupil mechanism of fly photoreceptors. *Vision Res.* **30**, 1235-1242.
- Smakman, J. G., van Hateren, J. H. and Stavenga, D. G.** (1984). Angular sensitivity of blowfly photoreceptors: Intracellular measurements and wave-optical predictions. *J. Comp. Physiol. A* **155**, 239-247.
- Snyder, A. W.** (1979). Physics of vision in compound eyes. In *Handbook of Sensory Physiology*, vol. VII/6A (ed. H. Autrum), pp. 225-313. Berlin, Heidelberg, New York: Springer.
- Stark, W. S., Ivanyshyn, A. M. and Greenberg, R. M.** (1977). Sensitivity of photopigments of R1-6, a two-peaked photoreceptor in *Drosophila*, *Calliphora* and *Musca*. *J. Comp. Physiol. A* **121**, 289-305.
- Stavenga, D. G.** (1979). Visual pigment processes and prolonged pupillary responses in insect photoreceptor cells. *Biophys. Struct. Mech.* **5**, 175-185.
- Stavenga, D. G.** (2002). Colour in the eyes of insects. *J. Comp. Physiol. A* **188**, 337-348.
- Stavenga, D. G.** (2003a). Angular and spectral sensitivity of fly photoreceptors. I. Integrated facet lens and rhabdomere optics. *J. Comp. Physiol. A* **189**, 1-17.
- Stavenga, D. G.** (2003b). Angular and spectral sensitivity of fly photoreceptors. II. Dependence on facet lens F-number and rhabdomere type. *J. Comp. Physiol. A* **189**, 189-202.
- Stavenga, D. G.** (2004). Angular and spectral sensitivity of fly photoreceptors. III. Dependence on the pupil mechanism in the blowfly *Calliphora*. *J. Comp. Physiol. A* **190**, 115-129.
- Stavenga, D. G., Kruijzinga, R. and Leertouwer, H. L.** (1990). Dioptrics of the facet lenses of male blowflies *Calliphora* and *Chrysomya*. *J. Comp. Physiol. A* **166**, 365-371.
- Stavenga, D. G., Smits, R. P. and Hoenders, B. J.** (1993). Simple exponential functions describing the absorbance bands of visual pigment spectra. *Vision Res.* **33**, 1011-1017.
- Stavenga, D. G., Oberwinkler, J. and Postma, M.** (2000). Modeling primary visual processes in insect photoreceptors. In *Molecular Mechanisms in Visual Transduction. Handbook of Biological Physics*, vol. 3 (ed. D. G. Stavenga, W. J. DeGrip and E. N. Pugh, Jr), pp. 527-574. Amsterdam: Elsevier.
- van Hateren, J. H.** (1984). Waveguide theory applied to optically measured angular sensitivities of fly photoreceptors. *J. Comp. Physiol. A* **154**, 761-771.
- Vogt, K. and Kirschfeld, K.** (1983). Sensitizing pigment in the fly. *Biophys. Struct. Mech.* **9**, 319-328.
- Vogt, K., Kirschfeld, K. and Stavenga, D. G.** (1982). Spectral effects of the pupil in fly photoreceptors. *J. Comp. Physiol. A* **146**, 145-152.